

Synthesis of antimicrobial silsesquioxane–silica hybrids by hydrolytic co-condensation of alkoxy silanes†

Cite this: *Polym. Chem.*, 2014, 5, 454

Shi-qiang Gong,^a D. Jeevanie Epasinghe,^b Wei Zhang,^a Bin Zhou,^a Li-na Niu,^c Heonjune Ryou,^d Ashraf A. Eid,^e Andrea Frassetto,^f Cynthia K. Y. Yiu,^b Dwayne D. Arola,^d Jing Mao,^{*a} David H. Pashley^g and Franklin R. Tay^{*g}

Organically modified silicates represent an excellent example of organic–inorganic hybrids in materials science. The routes to achieve incorporation of organic functionalities include grafting and co-condensation (one-pot synthesis). Compared with the grafting method, the advantage of one-pot synthesis manifests as the tunability of both mechanical and biological properties. Herein, we report a silsesquioxane–silica hybrid (SqSH) with dual functional groups (alkylammonium and methacrylate chains) synthesized by the hydrolytic co-condensation of one tetraethoxysilane and two alkoxy silanes. Successful co-condensation is validated by attenuated total reflection–Fourier transform infrared (ATR–FTIR), ²⁹Si nuclear magnetic resonance (²⁹Si NMR), and thermogravimetric analysis (TGA). 3–(Trimethoxysilyl) propyldimethyloctadecyl ammonium chloride (SiQAC), one of the three precursors, simultaneously serves as a structure-directing agent in the modified Stöber reaction, resulting in SqSH particles with structural hierarchy of both ordered lamellar structure and spherical morphology, as revealed by X-ray diffraction (XRD), scanning electron microscopy (SEM), and transmission electron microscopy (TEM). The SqSH particles bear tunable mechanical properties and, when incorporated into bis-GMA/TEGDMA resin, antimicrobial activities against *Streptococcus mutans*, *Actinomyces naeslundii*, and *Candida albicans*.

Received 17th May 2013
Accepted 13th August 2013

DOI: 10.1039/c3py00635b

www.rsc.org/polymers

Introduction

Organically modified silicates are organic–inorganic hybrid materials in which the organic moieties are covalently linked to the siloxane backbone.¹ Their rheological behavior may be modified by varying the precursor ratios, resulting in materials exhibiting rubbery or brittle characteristics.² Silsesquioxanes ([RSiO_{1.5}]_n) are specific examples of organically modified silicates in which R is hydrogen or any organic group (*e.g.*, alkyl, alkylene, aryl, *etc.*).

Silsesquioxanes or silsesquioxane–silica hybrids are synthesized using a Stöber-like sol–gel route,³ *via* hydrolytic condensation of trialkoxy silanes, bridged alkoxides or co-condensation between a tetra-alkoxy silane and a trialkoxy silane.^{4–6} By controlling the organic–inorganic composition, as well as functionality of these hybrid materials, a wide variety of silicate-based hybrid materials may be produced for applications in the fields of catalysis,⁴ optical devices,⁷ coating and polymer science.^{8,9}

The introduction of reactive functionalities into silsesquioxanes may be achieved *via* post-synthetic surface functionalization procedures (grafting), which are based upon the chemical reaction of silica particles with coupling agents bearing organic functional groups. However, the limitations of the grafting method are that there are relatively few silanol groups available on the surface of the silica particles and the procedure is time-consuming. In addition, this method generally results in particles containing only one type of functional group. Direct synthesis, in which silica-based hybrid particles are generated by the co-condensation of tetra-alkoxy silane with terminal trialkoxy silane, represents a more advantageous route, with the organic functionality distributed within the synthesized materials instead of the surface of the materials.^{10–13} In addition, the organic functionalities are more homogeneously distributed during the co-condensation process, when compared with materials that are produced by the grafting method. This is

^aDepartment of Stomatology, Tongji Hospital, Tongji Medical College, Huazhong University of Science and Technology, Wuhan, China. E-mail: maojing@mail.hust.edu.cn

^bPediatric Dentistry and Orthodontics, The University of Hong Kong, Hong Kong SAR, China

^cSchool of Stomatology, Fourth Military Medical University, Xi'an, China

^dDepartment of Mechanical Engineering, University of Maryland Baltimore County, Baltimore, Maryland, USA

^eNagasaki University, Nagasaki, Japan

^fUniversity of Trieste, Trieste and IGM-CNR, Bologna, Italy

^gCollege of Dental Medicine, Georgia Regents University, Augusta, Georgia, USA. E-mail: tayfranklin7@gmail.com

† Electronic supplementary information (ESI) available: Co-condensation reaction scheme, FTIR and TG analyses, TEM image from peanut-like structures of SqSHs with partial coalescence, STEM-EDX images of SqSH 1-32-1, cytotoxicity of SqSHs and sol–gel silica particles. See DOI: 10.1039/c3py00635b

especially so in the case of fabricating mesoporous structures in which organic functionalization of the center of the pores through the grafting method may be impaired as a result of the pore blocking effect if the organosilanes react preferentially at pore openings. It is generally believed that periodic mesoporous organosilica particulates that are produced *via* hydrolysis and condensation reactions of bridged organosilica precursors have a higher degree of homogeneity of the organic functionalities.⁴ Despite ample reports of such a method, the literature is sparse in the synthesis of silica-based hybrids containing dual functional groups.

Recently, efforts have been made to explore the ability of organosilanes with surfactant chain-bearing groups to self-direct the hydrolysis and condensation of alkoxy silane precursors into structures with mesoporous characteristics.^{14–17} Although the mechanisms of using surfactant silanes to facilitate the formation of particles with tailored mesostructures (*i.e.*, mesoporous,^{14,15} lamellar,^{15,16} and worm-like mesostructures¹⁶) were well understood, little is known regarding the synthesis of mesostructured hybrid materials with dual functionalities. Here, we report a modified Stöber route for synthesizing silsesquioxane–silica hybrid (SqSH) particles by the hydrolytic co-condensation of tetraethoxysilane (TEOS) with two trialkoxysilanes: 3-(trimethoxysilyl)propyldimethyloctadecyl ammonium chloride (SiQAC) and 3-methacryloxypropyltrimethoxysilane (3-MPTS), without the use of an additional surfactant. The alkylammonium chain from

SiQAC is responsible for its antimicrobial potential,¹⁸ and serves as a structure-directing agent (*i.e.* surfactant silane) during the co-condensation process.¹⁹ The dual roles of SiQAC as a surfactant silane and the contributor of the antimicrobial functionality eliminate the need for surfactant removal after synthesis, thereby avoiding the risk of destroying the other organic functionality (*i.e.* methacrylate groups from 3-MPTS) during the removal of surfactant by extractive or calcination methods. In this one-pot synthesis, the molar ratio of SiQAC and 3-MPTS was maintained at 1 : 1, while the molar ratio of TEOS varied from 1 to 32, resulting in silsesquioxane–silica hybrids (SqSHs) with overall molar ratios of 1 : 1 : 1, 1 : 2 : 1, 1 : 4 : 1, 1 : 8 : 1, 1 : 16 : 1 and 1 : 32 : 1. The sol-gel hydrolytic condensation product of TEOS was used as a control (sol-gel silica) [ESI S1†].

Results and discussion

Synthesis of SqSH particles by hydrolytic co-condensation and characterization

An issue that confronts silane-based co-condensation reactions is homocondensation of the trialkoxysilanes.²⁰ Thus, the products of the sol-gel reactions were subjected to multiple washings in ethanol prior to analyses to remove unreacted reagents. Attenuated total reflection-Fourier transform infrared (ATR-FTIR) spectroscopy validates the presence of both the methacrylate group at 1690–1714 cm^{-1} (C=O), 1637 cm^{-1} (C=C), 1305 cm^{-1} (C–CO–O),

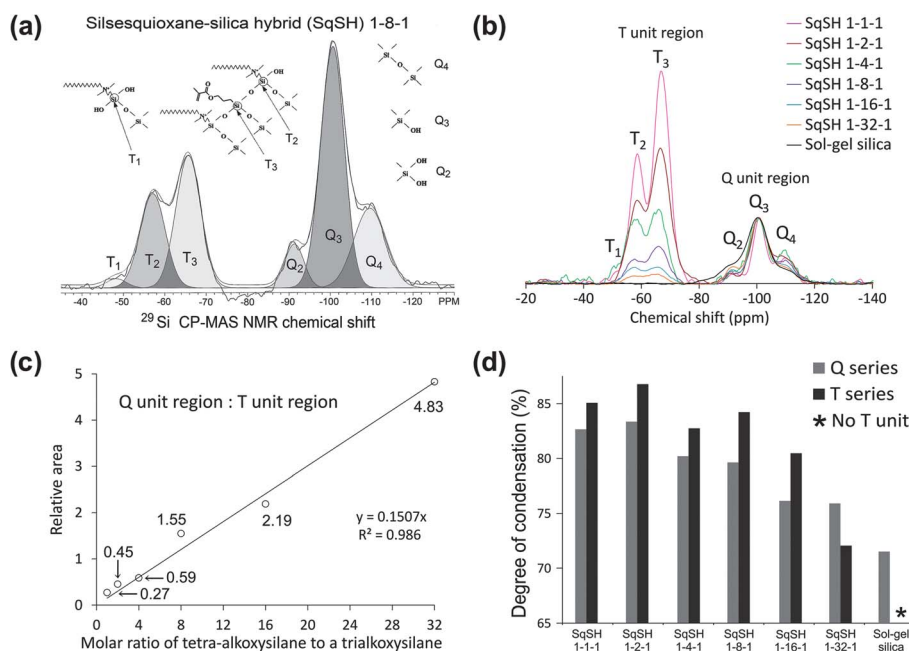


Fig. 1 (a) Representative ²⁹Si CP-MAS NMR spectrum of a silsesquioxane–silica hybrid (SqSH) 1-8-1 revealing two different units: T units are derived from trialkoxysilane (3-MPTS or SiQAC), and Q units from TEOS. T_n and Q_n represent silicon entities with different bonding environments derived from RSi(OH)_(3–n)(OSi)_n and Si(OH)_(4–n)(OSi)_n, respectively. For any T_n or Q_n unit, the relative area (T_n or Q_n unit region) is shown as an individual gray-filled region deconvoluted from the spectrum. (b) Overlay of ²⁹Si CP-MAS NMR spectra of SqSHs and sol-gel silica, normalized to their respective Q₃ units. The relative areas of T units increase as a function of composition of trialkoxysilane (3-MPTS and SiQAC) in SqSHs, while the T unit in sol-gel silica derived from TEOS only. (c) A linear regression model provides an excellent fit ($R^2 = 0.986$; $P < 0.001$) for the relation between the ratio of Q unit region to T unit region and the molar ratio of tetraethoxysilane to a trialkoxysilane. (d) The degree of condensation of Q or T units improves with increased molar ratios of the trialkoxysilanes (3-MPTS and SiQAC) in the SqSHs, except that the degree of condensation of SqSH 1-1-1 is slightly less than that of SqSH 1-2-1.

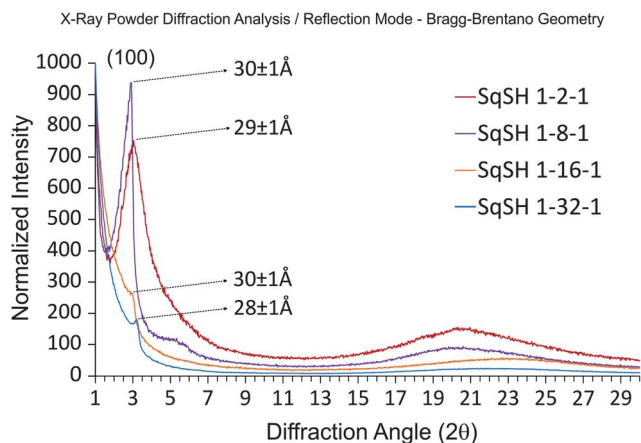


Fig. 2 Powder X-ray diffraction patterns of SqSHs 1-2-1, 1-8-1, 1-16-1, and 1-32-1.

1295 cm^{-1} (C–CO–O),²¹ 815 cm^{-1} (C=C)) and the alkylammonium chain (1373 cm^{-1} (C–N)²²) in the sol-gel reaction products [ESI S2†], thereby confirming the co-condensation of TEOS with 3-MPTS and SiQAC in the multiple-rinsed reaction products.

Using ^{29}Si cross-polarization-magic angle spinning nuclear magnetic resonance (CP-MAS NMR) spectroscopy, two different units were delineated from the NMR spectrum, providing information on the connectivity of the silica network:²³ $\text{T}_n\text{-RSi}(\text{OH})_{(3-n)}(\text{OSi})_n$, and $\text{Q}_n\text{-Si}(\text{OH})_{(4-n)}(\text{OSi})_n$ (Fig. 1a). As shown by the overlay of the NMR spectra of SqSHs and inorganic sol-gel silica synthesized by the Stöber method, with all spectra normalized to the Q_3 unit, the relative areas of the T unit region increase linearly as a function of the feed ratio of trialkoxysilanes (3-MPTS and SiQAC) to TEOS (Fig. 1b and c). The degree of condensation of Q or T units, as determined by the ratios of the relative areas for different Q or T silicon connections,²⁴ improves with increased concentration of trialkoxysilane (3-MPTS or SiQAC) in the SqSHs (Fig. 1d). This is in agreement with the ATR-FTIR results [ESI S2†], wherein cyclic Si–O–Si ($\sim 1080\text{ cm}^{-1}$)²⁵ is apparent only in SqSH 1-1-1 and SqSH 1-2-1, both containing high organic components in the organosilica hybrids. Interestingly, while T_3 (fully condensed trimeric species) dominates in the T units, all SqSHs as well as sol-gel silica present a large amount of Q_3 species bearing one hydroxyl group. This may be explained by the reasoning that hydrolyzed TEOS bearing four hydroxyl groups has more steric hindrance during condensation, compared with trialkoxysilanes with three hydroxyl groups. Thermogravimetric analysis (TGA) was performed to further characterize the synthesized SqSHs [ESI S3†]. The post-calcination residual inorganic mass increases with increasing feed ratios of TEOS to the trialkoxysilanes (3-MPTS and SiQAC), which is consistent with the ^{29}Si NMR results.

By changing the feed ratios of TEOS to the trialkoxysilanes, ordered structures with variable d spacings within the spherical particles could be discerned by XRD and electron microscopy. The SiQAC molecule contains a long hydrophobic alkyl chain linked to the silicon atom by a Si–C bond, which is chemically stable under hydrolytic conditions. It becomes amphiphilic when silanol groups are formed during hydrolysis.²⁶ Based on

this amphiphilic assembly mechanism, lamellar mesostructures may be produced inside the hybrid silica particles within two hours using the Stöber route with a strong base (ammonium hydroxide) as the catalyst. Small angle powder X-ray diffraction (XRD) patterns of the SqSH 1- n -1 ($n = 2, 8, 16$, and 32) show diffraction peaks corresponding to the d spacing value of $2.9 \pm 0.1\text{ nm}$ (Fig. 2). One should note that these d values are smaller than those identified from condensed alkoxy silanes with bilayer lamellar structure ($d = 5.3\text{ nm}$),²⁷ indicating a different molecular packing profile. Diffraction peak intensity becomes higher with the increased ratio of TEOS to SiQAC for SqSH 1- n -1 where $n \leq 8$. This implies that addition of increased concentrations of TEOS with strong three-dimensional network formation ability leads to more highly ordered siloxane networks with reduced mesoporosity.

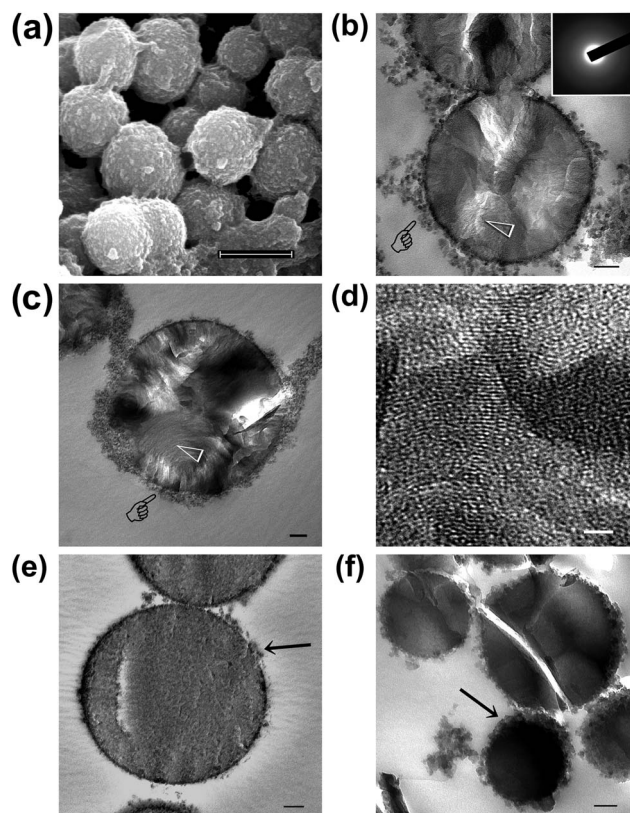


Fig. 3 (a) Representative scanning electron microscopy image taken from SqSH 1-8-1. Scale bar: 200 nm. (b) Transmission electron microscopy (TEM) image showing non-sintered SqSH 1-2-1 particles with uneven electron density inside. Scale bar: 50 nm. Inset: selected area electron diffraction revealed the amorphous nature of the SqSH particles. (c) TEM showing the SqSH 1-2-1 particles after calcination, with uneven distribution of silica (organic components are removed after calcination) inside the particles, and circumferential particulates that are formed on the surface of the particles (pointer). Scale bar: 50 nm. (d) High magnification TEM showing the lamellar structure inside the SqSH 1-2-1 particles (open arrowheads in b and c). Scale bar: 20 nm. (e) TEM of SqSH 1-32-1 showing even electron density distribution inside the particles. Particulate precipitations are attached along the particle surface (arrows in e and f). Scale bar: 50 nm. (f) TEM showing increased electron density within the SqSH 1-32-1 particles after calcination, caused by the removal of organic components and possible collapse of any pre-existing intra-lamellar spaces. Fracture is an artifact of sectioning. Scale bar: 50 nm.

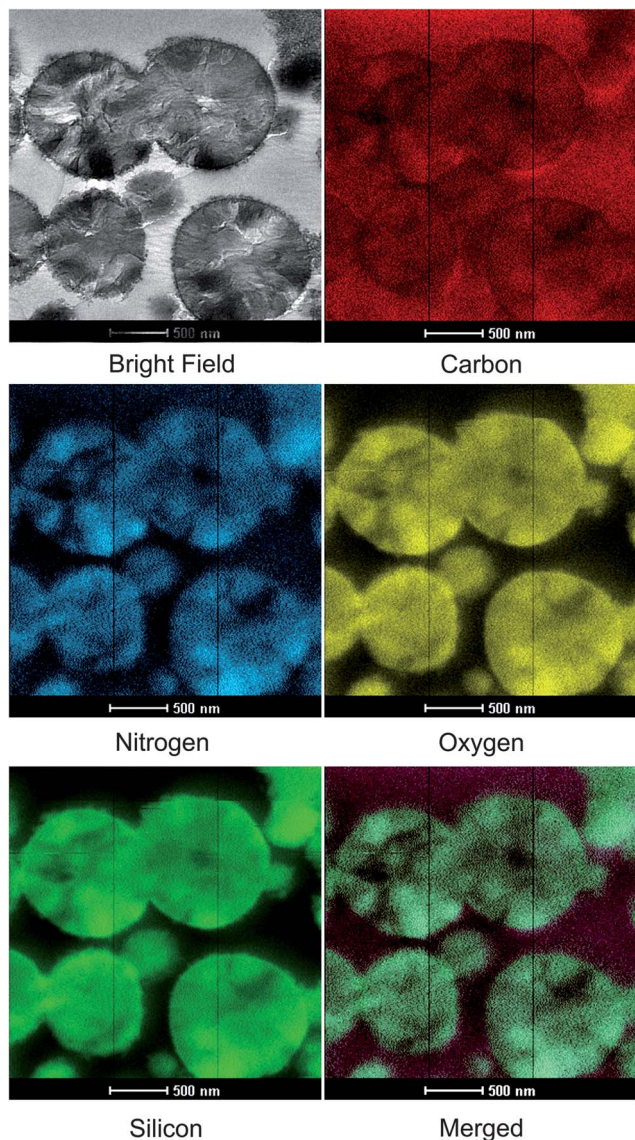


Fig. 4 Scanning transmission electron microscopy-energy dispersive X-ray elemental mappings of the distribution of carbon, nitrogen, oxygen, and silicon within SqSH 1-8-1 particles.

Incorporation of tetraalkoxysilane in the self-assembly process of alkyltrialkoxysilane also contributes to the increase of the thermal stability, a feature that could not be attained by hydrolysis and condensation of alkyltrialkoxysilane alone.²⁸ The network-forming ability of TEOS was also verified by the observation that no particles were formed from the hydrolytic co-condensation of the two trialkoxysilanes (SiQAC and 3-MPTS) in the absence of TEOS, under the present experimental conditions.

Sol-gel silica particles synthesized by the hydrolysis and condensation reactions of TEOS alone in the present study are monodisperse (~200 nm in diameter; data not shown), whereas the SqSH particles are slightly larger (*ca.* 250–1000 nm) and polydisperse, as revealed by scanning electron microscopy (SEM) (Fig. 3a). The SqSH particles exhibited a tendency to partially coalesce prior to solidification into particulates, producing peanut-like structures [ESI S4[†]]. The morphology

of these partially coalesced SqSH particles is similar to the morphology of previously reported particles prepared from the co-condensation of TEOS with aminopropyltriethoxysilane (APTES) *via* a Stöber-like route.¹² Unlike the TEOS-derived spherical silica particles which have smooth surfaces, the surfaces of the SqSH particles are rough, as observed using transmission electron microscopy (TEM), with small aggregates forming around the SqSH particle even after multiple ethanol rinses (Fig. 3b). These surface aggregates are possibly formed by the self-condensation of SiQAC or 3-MPTS that are covalently bonded to the SqSH surface, as they were resistant to ethanol rinsing and sonication, and became sparser after calcination (Fig. 3c). For SqSH 1-*n*-1 ($n \leq 8$), lamellar structures can be discerned by TEM at high magnification (Fig. 3d). For SqSH 1-*n*-1 ($n > 8$) lamellar structures cannot be identified by TEM (Fig. 3e); the SqSH particles became solid spheres after calcination (Fig. 3f).

The presence of silicon, oxygen, nitrogen and carbon within SqSH 1-8-1 and SqSH 1-32-1 particles was confirmed using scanning transmission electron microscopy-energy dispersive X-ray analysis (STEM-EDX; Fig. 4 and ESI S5[†]). Identification of nitrogen within the SqSH particles is indicative of the presence of the quaternary ammonium functionality (derived from SiQAC) within the entire particle. This is contrary to a grafting procedure in which the quaternary ammonium functionality is only present along the particle surface. The STEM-EDX data, however, do not permit conclusions to be drawn with respect to the methacryloxy functionality derived from 3-MPTS.

Mechanical properties of SqSH particles

Silsesquioxane-silica hybrids with different organic-inorganic compositions and variable structures should be modifiable in terms of mechanical and biological properties. The mechanical properties of SqSHs can be tuned by altering the TEOS molar feed ratio, so that particles with higher silica content can be produced. Nanoindentation performed on SqSH particles and sol-gel silica using the method reported by Oliver and Pharr²⁹ revealed correlations between increases in reduced modulus and hardness, with increasing feed ratios of TEOS to the trialkoxysilane (Fig. 5).

Antimicrobial activities of SqSH incorporated bis-GMA/TEGDMA resins

Because SqSHs bearing methacryloxy functional groups can be co-polymerized with methacrylate resin in the presence of certain catalysts (*e.g.* photoinitiator and tertiary amine accelerator), SqSHs with different TEOS-trialkoxysilane molar feed ratios are added into a resin blend consisting of 2,2-bis[4-(2-hydroxy-3-methacryloxypropoxy)phenyl]propane (bis-GMA) and triethylene glycol dimethacrylate (TEGDMA), with camphorquinone (CQ) and ethyl(4-dimethylamino)benzoate (EDMAB) as the photoinitiator and accelerator, respectively. Incorporation of the SqSH organic-inorganic hybrid particles into the methacrylate resin blend results in a series of antimicrobial resin composites that may be used for restoring teeth and preventing recurrent decay caused by colonization of bacterial biofilms around the margins of the tooth fillings.

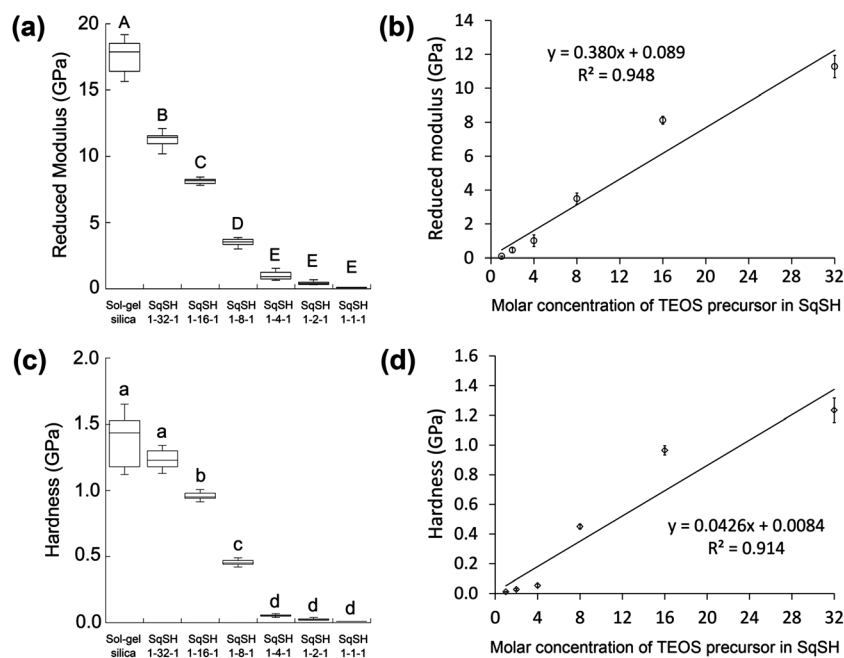


Fig. 5 Reduced modulus and hardness measurements obtained from nanoindentation of SqSH particles and sol-gel silica. (a) Reduced modulus ($n = 6$). Groups labeled with the same upper case letters are not statistically significant ($P > 0.05$). Error bar represents standard deviation. (b) Linear regression model demonstrates a significant relation ($R^2 = 0.948$; $P < 0.05$) between the reduced modulus and the molar ratio of tetraethoxysilane to one of the two trialkoxysilanes. (c) Hardness ($n = 6$). Groups labeled with the same lower case letters are not statistically significant ($P > 0.05$). Error bar represents standard deviation. (d) Linear regression model demonstrates a significant relation ($R^2 = 0.914$; $P < 0.05$) between the hardness and the molar ratio of tetraethoxysilane to one of the two trialkoxysilanes.

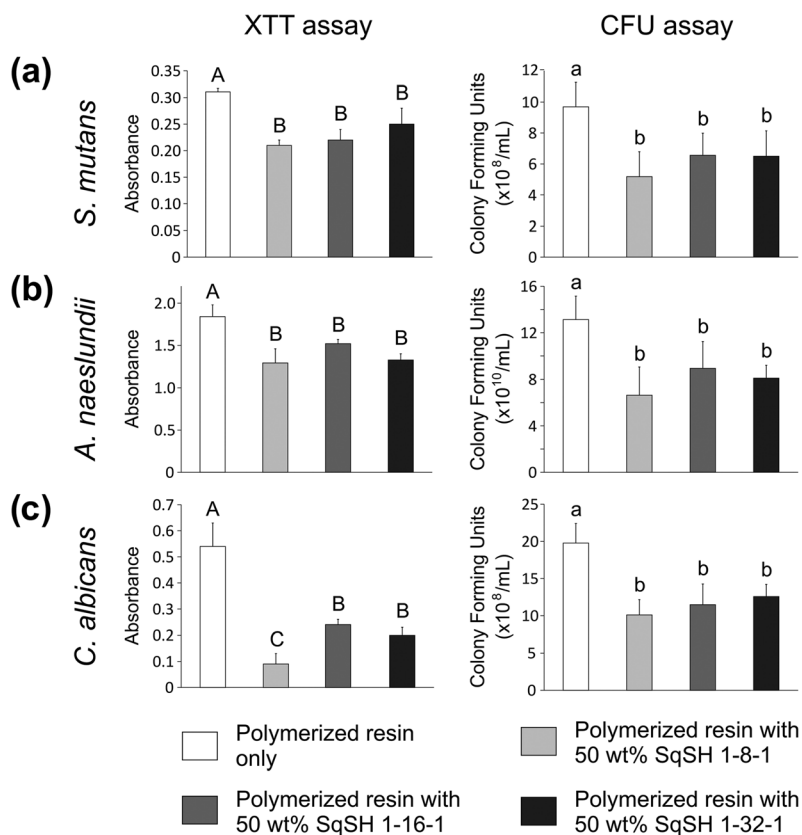


Fig. 6 Antimicrobial activities of polymerized bis-GMA/TEGDMA resin containing SqSHs, as assessed by XTT and CFU assays. (a) *S. mutans*. (b) *A. naeslundii*. (c) *C. albicans*. For each microbe species, groups labeled with the same letters (upper case letters for XTT assay and lower case letters for CFU assay) are not statistically significant ($P > 0.05$).

Three SqSH-containing resin composites (SqSH 1-8-1, 1-16-1 and 1-32-1) were chosen in the present study due to their relatively high reduced modulus and hardness, when compared to sol-gel silica, which are desirable properties for preparing restorative resin composites. Previous studies have demonstrated that incorporation of SiQAC-derived sol-gel reaction products confers resinous materials with antimicrobial activities against bacteria and fungi.^{30,31} The antimicrobial potential of SqSH-containing methacrylate resins against *Streptococcus mutans*, *Actinomyces naeslundii*, and *Candida albicans* were confirmed using 2,3-bis-(2-methoxy-4-nitro-5-sulphophenyl)-2H-tetrazolium-5-carboxanilide (XTT) and Colony Forming Unit (CFU) assays (Fig. 6). *Streptococcus mutans* and *A. naeslundii* are cariogenic oral pathogens, while *C. albicans* is associated with oral candidiasis in susceptible hosts. It is likely that the antimicrobial activities of SqSH containing methacrylate resins are permanent and non-leaching,³¹ as SqSH particles are copolymerized with the methacrylate network. This non-leaching antimicrobial activity is independent of the loss of surface layer of the composite by wear during function, since SqSH particles are dispersed throughout the bulk resin matrix.

Because materials that possess antimicrobial properties against bacteria or fungi may be toxic to mammalian cells, we performed 3-(4,5-dimethylthiazol-2-yl)-2,5-diphenyltetrazolium bromide (MTT) assay on a mouse fibroblast cell line (L929) to examine the effects of increasing molar feed ratios of SiQAC on the cytotoxicity of SqSHs (ESI S6†). The results demonstrate a significant positive correlation between the 50% reduction in cell viability (IC_{50}) of the mammalian cells and the molar feed ratio of TEOS employed for the synthesis of the SqSH particles.

Mesoporous antimicrobial SqSH particles with spherical morphology and lamellar structures may also be used as absorbents or carriers for loading bioactive agents, such as growth factors, catalysts, metal ions, and photoactive molecules, to

achieve other functions. Other alkoxy-silanes with different organofunctional moieties (*e.g.*, vinyl, epoxy, isocyanato, sulfonate, carboxylate, *etc.*) may be used *in lieu* of 3-MPTS, enabling these hybrid particles to satisfy different product requirements. The versatile functionality of these hybrid materials will expand the range of their applications in various fields. For example, antimicrobial SqSH particles containing acrylate functionalities may be incorporated into acrylate-based paints; antimicrobial SqSH particles containing vinyl functionalities may be blended with polypropylene *via* an extruder to produce antimicrobial food wraps for the food industry.

Conclusions

We have developed a facile method for synthesizing unique SqSH particles *via* a Stöber-like approach, with ordered lamellar structures with spherical morphology, without the use of additional surfactants. A scheme illustrating the influence of surfactant and formation of SqSH nanospheres is shown in Fig. 7. This one-pot synthesis approach leads to the development of unique and useful antimicrobial hybrid silica particles with quaternary ammonium groups distributed within the entire particles, and therefore, non-leaching antimicrobial activities, as opposed to a grafting procedure, where this type of functionality is present only along the particle surface. Moreover, antimicrobial activities are present irrespective of the degree of mesoscopic order of the hybrid silica particles. This synthesis approach may be further expanded by replacing the methacrylate functionality with other organofunctional moieties, thereby enabling the antimicrobial hybrid particles with tunable mechanical properties to be incorporated into different polymers/copolymers for a wide range of commercial applications.

Materials and methods

Chemicals and reagents

Tetraethoxysilane (TEOS), 3-(trimethoxysilyl)propyldimethyloctadecyl ammonium chloride (SiQAC), 3-methacryloxypropyltrimethoxysilane (3-MPTS), ammonium hydroxide solution (28–30% NH_3), triethylene glycol dimethacrylate (TEGDMA), ethyl(4-dimethylamino)benzoate (EDMAB) and camphorquinone (CQ) were purchased from Sigma-Aldrich (St Louis, MN, USA) and used without further purification. The SiQAC was supplied at 72 wt% in methanol. 2,2-Bis[4-(2-hydroxy-3-methacryloxypropoxy)phenyl]propane (bis-GMA) was a gift from Esstech, Inc. (Essington, PA, USA).

Co-condensation procedure

The molar ratio of SiQAC and 3-MPTS was maintained at 1 : 1, while the molar ratio of TEOS varied from 1 to 32, resulting in silsesquioxane-silica hybrids (SqSHs) with overall molar ratios of 1 : 1 : 1, 1 : 2 : 1, 1 : 4 : 1, 1 : 8 : 1, 1 : 16 : 1 and 1 : 32 : 1 (Fig. S1†). The sol-gel hydrolysis/condensation product of TEOS was used as the control (sol-gel silica). Co-condensation was processed *via* a modified Stöber route:³ 16 mL of ethanol, 25 mL of deionized water, and 9 mL of NH_4OH solution were mixed and stirred at 1200 rpm. To this solution, 5 mL of TEOS, or

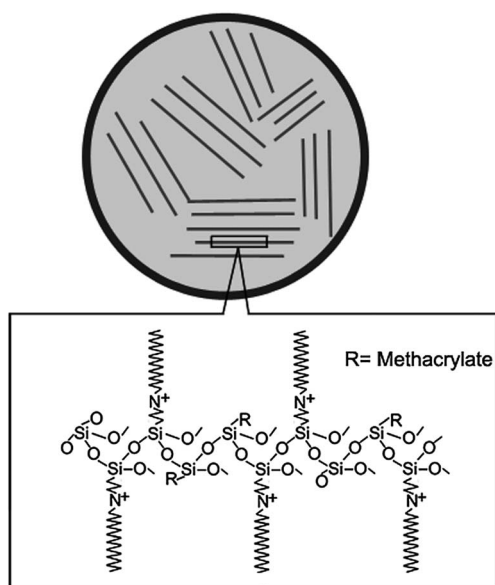


Fig. 7 Schematic illustration of SqSH particles with structural hierarchy of both ordered lamellar structure and spherical morphology.

SiQAC-3-MPTS-TEOS premixed in 45 mL of ethanol, was rapidly added. After 1 min, the stirring speed was reduced to 350 rpm. The reaction was maintained at room temperature for 2 hours. The product was then centrifuged and washed with copious amounts of water and ethanol. The procedures were repeated three times before the reaction products were dried under vacuum. The yield varied from 55 to 86 wt%. The yield of the SqSHs varied with respect to the molar ratio of the trialkoxysilane (*i.e.* high proportion of trialkoxysilane decreased the yield rate). Due to the different hydrolysis and condensation kinetics of the structurally different precursors, a relatively higher proportion of trialkoxysilane in the reaction mixture favors homocondensation reactions of the trialkoxysilanes, at the expense of co-condensation with the inorganic silica precursor (TEOS). This accounts for the wide variety in yields among the SqSHs prepared with different molar ratios of the precursors after ethanol extraction of the homocondensation reaction products.

Attenuated total reflection-Fourier transform infrared (FTIR) spectroscopy

Infrared spectra were recorded between 4000 and 400 cm^{-1} using a Fourier-transform infrared spectrometer (Nicolet 6700, Thermo Scientific, Waltham, MA, USA) with an attenuated total reflection (ATR) set up at a resolution of 4 cm^{-1} and averaging 32 scans per spectrum.

Nuclear magnetic resonance (NMR) characterization

The structures of SqSHs and sol-gel silica were characterized by ^{29}Si solid-state NMR at ambient temperature using a 270 MHz spectrometer (JEOL, Tokyo, Japan) equipped with a 7 mm Magic Angle Spinning (MAS) probe. Spectra were acquired in the $^1\text{H} \rightarrow ^{29}\text{Si}$ cross-polarization (CP) mode, using a MAS frequency of 4 kHz, with a 45 degree pulse angle of 5 μs . The ^1H Larmor frequency for ^{29}Si was 53.76 MHz. Chemical shifts were referenced to external tetramethylsilane (TMS) at 0 ppm.

Thermogravimetric analysis (TGA)

TGA was performed with a Q500 thermogravimetric analyzer (TA Instruments, New Castle, DE, USA). Approximately 40 mg of dried particles (SqSHs or sol-gel silica) was placed in individual platinum pans and heated at a rate of 10 $^{\circ}\text{C min}^{-1}$ to 1000 $^{\circ}\text{C}$ in atmospheric air. The data were analyzed using Universal Analysis 2000 software (TA Instruments) and expressed as weight *vs.* temperature as well as derivative weight *vs.* temperature.

Powder X-ray diffraction (XRD)

X-ray diffraction (Rigaku America, Woodlands, TX, USA) of the non-sintered particles was performed using Ni-filtered Cu $K\alpha$ radiation (30 KeV, 20 mA), in the 2θ range of 1–30 $^{\circ}$, with a scan rate of 4 $^{\circ}$ per min, and a sampling interval of 0.02 $^{\circ}$. The determination of d -spacing values was based on the Bragg-Brentano geometry.

Electron microscopy

Dried particles sputter-coated with gold/palladium were examined using a field emission-scanning electron microscope (XL-30 FEG; Philips, Eindhoven, The Netherlands) operating at 10–15 kV. Dried particles were embedded in epoxy resin and cut into 70–90 nm thick sections. Unstained sections were examined using a JSM-1230 transmission electron microscope (JEOL, Tokyo, Japan) at 110 kV. Selected area electron diffraction (SAED) was performed to identify the crystallinity of the SqSH particles.

Scanning transmission Electron microscopy-energy dispersive X-ray (STEM-EDX) analysis

Elemental analysis of representative SqSH 1-8-1 and 1-32-1 was performed on unstained thin sections prepared previously for TEM using a Tecnai G2 STEM (FEI, Hillsboro, OR, USA) at 200 kV. Spectrum acquisition and elemental mapping were conducted using an Oxford Instruments INCA x-sight detector. Images were collected with a Gatan 1 K \times 1 K CCD camera. Elemental mappings were acquired with FEI TIA software using a spot dwell time of 300 msec. As each 250 \times 250 pixel mapping required 7 hours to complete, drift correction was performed after every 30 images.

Nanoindentation

Cold-polymerized epoxy resin with embedded SqSH or sol-gel silica particles was sectioned with a water-cooled diamond-impregnated blasé to expose the particles along the flat resin surface. Mechanical properties of the specimens were evaluated by quasi-static indentation using a nanoindenter (Hysitron Tribindenter 900, Minneapolis, MN, USA) with a 100 nm radius cono-spherical diamond tip indenter. A standard trapezoidal profile was used including a maximum load of 100 mN, indentation hold time of 5 s, and loading and unloading rates of 20 mN s^{-1} . An initial offset load of 10 mN was used for identifying contact and initializing the indentation process. The load-displacement curves generated for the individual indentations were corrected for the offset force. Six indentations were performed to characterize the mechanical behavior of each SqSH or sol-gel silica control ($N = 6$). Reduced modulus and hardness (in GPa) were calculated based on the Oliver-Pharr method for nanoindentation testing.²⁹ Data were analyzed using one-way ANOVA with Tukey's multiple comparison at $\alpha = 0.05$.

Antimicrobial activities of bis-GMA/TEGDMA resin containing SqSH

A bis-GMA/TEGDMA light-polymerizable resin blend (composition: 70 wt% bis-GMA, 28.5 wt% TEGDMA, 1 wt% EDMAB and 0.5 wt% CQ) was used to mix with 50 wt% SqSH particles in a centrifugal mixing device at 3200 rpm for 60 s (DAC 150 Speedmixer; FlackTek Inc., Landrum, SC, USA). Bis-GMA/TEGDMA resin without any SqSH was used as the control. Polymerization of these resins was achieved by photocuring with visible light in the wavelength range of 410–500 nm. With a Teflon mold and Mylar sheets covering both sides, polymerized

resin disks (6 ± 0.1 mm diameter, 1 ± 0.1 mm thick) were fabricated.

Streptococcus mutans ATCC 35668 (ATCC, Manassas, VA, USA) and *Actinomyces naeslundii* ATCC 12104 were cultured in Brain Heart Infusion (BHI) broth (Difco, Becton-Dickinson and Co., Sparks, MD, USA), supplemented with 50 mM sucrose (pH 7.2). *Candida albicans* ATCC 90028 was cultured in Yeast Nitrogen Base (YNB; Difco) supplemented with 50 mM glucose (pH 7.2). Harvested cells were re-suspended in 100 mL of the respective growth medium, and adjusted to a concentration of 10^7 CFU mL⁻¹ before use. Each microbe was used individually for the formation of single-species biofilms on salivary pellicle-coated resin disks inside an oral biofilm reactor. After the formation of biofilms on acrylic surfaces, half of the disks from each group were transferred carefully into separate microtubes containing 4 mL of phosphate buffered saline (PBS; 0.01 mM, pH 7.3), avoiding any disturbances to the biofilms. Fifty mL of 1 mg mL⁻¹ solution of 2,3-bis-(2-methoxy-4-nitro-5-sulphophenyl)-2H-tetrazolium-5-carboxanilide (XTT; Sigma-Aldrich) was then added to each microtube, together with 4 μ L of 1 mM menadione (Sigma-Aldrich). The solutions were mixed gently, covered with aluminum foil, and incubated for 5 h at 37 °C. After incubation, the solution was transferred to a new microtube and centrifuged at 4000 rpm for 10 min at 4 °C. The supernatant was placed in a 96-well plate and read at 492 nm using a spectrophotometer (Victor, R & D systems, Minnesota, USA).

The rest of the disks from each group were placed carefully in separate microtubes containing 1 mL of PBS and vortexed (Maxi Mix vortex mixer, Thermo Scientific, Waltham, MA, USA) for 2 min at high speed to detach the biofilm. Ten-fold serial dilutions were generated in PBS (0.01 mM, pH 7.3), and each dilution was plated (50 μ L aliquots) onto Sabouraud Dextrose Agar plates for *C. albicans*, and Brain Heart Infusion agar plates for *S. mutans* and *A. naeslundii*. The plates were incubated at 37 °C for 48 h in an aerobic chamber for *C. albicans* and anaerobic chamber for *S. mutans* and *A. naeslundii*. After incubation, the colony forming unit counts (CFUs) per resin disk were counted manually. Data were analyzed using one-way ANOVA with Tukey's multiple comparison at $\alpha = 0.05$.

Cytotoxicity

The cytotoxicity of SqSHs and sol-gel silica was investigated using a mouse fibroblast cell line (L-929). The growth medium for L-929 consisted of Dulbecco's Modified Eagle's Medium (DMEM, Lonza, Walkersville, MD, USA) and 10% fetal bovine serum (Gibco; Invitrogen Corp., Carlsbad, CA, USA), supplemented with 2 mM L-glutamine, 100 U per mL penicillin, and 100 μ g mL⁻¹ streptomycin. The cells were plated in a 96-well plate at a density of 5000 cells per cm², in 200 μ L of the growth medium, and incubated at 37 °C in a humidified 5% CO₂ atmosphere. After 24 hours, pre-confluent cells were washed twice with serum or antibiotics free DMEM and further incubated in DMEM containing SqSH or silica particles at different concentrations. Cells incubated in growth medium without particles were used as the blank control.

The final SqSH or silica dispersions in DMEM were prepared immediately before use by serial dilution (*i.e.*, 2, 5, 25, 125, 625, and 3125 folds) of the stock suspension (*ca.* 883 μ g mL⁻¹) with intense vortexing.

Succinic dehydrogenase (SDH) activity of the cells was determined using 3-(4,5-dimethylthiazol-2-yl)-2,5-diphenyltetrazolium bromide (MTT) assay. The retrieved cells were incubated in MTT-succinate solution for 60 min and fixed with Tris-formalin. The formazan product was dissolved *in situ* using DMSO and absorbance was recorded using a microplate reader at 562 nm. Results were determined as a percentage of mean control values. The half-maximal inhibitory concentration (IC₅₀) was defined as the concentration of SqSH or silica particles leading to a 50% reduction in L-929 cell viability.³² It was determined by linear regression analysis of the logarithmic derivative of particle concentration *vs.* reduction of cell viability using SPSS 16.0 (SPSS Inc., Chicago, IL, USA).

Acknowledgements

The authors thank Frankie Chan, the University of Hong Kong, for performing the STEM-EDX analysis, and Michelle Barnes, Georgia Regents University, for secretarial support.

Notes and references

- 1 L. Nicole, L. Rozes and C. Sanchez, *Adv. Mater.*, 2010, **22**, 3208.
- 2 J. D. Mackenzie, Y. J. Chung and Y. Hu, *J. Non-Cryst. Solids*, 1992, **147–148**, 271.
- 3 W. Stöber, A. Fink and E. Bohn, *J. Colloid Interface Sci.*, 1968, **26**, 62.
- 4 F. Hoffmann, M. Cornelius, J. Morell and M. Fröba, *Angew. Chem., Int. Ed.*, 2006, **45**, 3216.
- 5 H. Mori, Y. Miyamura and T. Endo, *Langmuir*, 2007, **23**, 9014.
- 6 E. Ruiz-Hitzky, P. Aranda, M. Darder and M. Ogawa, *Chem. Soc. Rev.*, 2011, **40**, 801.
- 7 C. Sanchez, B. Lebeau, F. Chaput and J. P. Boilot, *Adv. Mater.*, 2003, **15**, 1969.
- 8 X. X. Zhang, B. B. Xia, H. P. Ye, Y. L. Zhang, B. Zhao, L. H. Yan, H. B. Lv and B. Jiang, *J. Mater. Chem.*, 2012, **22**, 13132.
- 9 B. M. Novak, *Adv. Mater.*, 1993, **5**, 422.
- 10 A. Van Blaaderen and A. Vrij, *J. Colloid Interface Sci.*, 1993, **156**, 1.
- 11 C. R. Silva and C. Airoidi, *J. Colloid Interface Sci.*, 1997, **195**, 381.
- 12 S. Chen, S. Hayakawa, Y. Shirosaka, E. Fujii, K. Kawabata, K. Tsuru and A. Osaka, *J. Am. Ceram. Soc.*, 2009, **92**, 2074.
- 13 Y. Naka, Y. Komori and H. Yashitake, *Colloids Surf., A*, 2010, **36**, 162.
- 14 G. Büchel, K. Klaus, K. K. Unger, A. Matsumoto and K. Tsutsumi, *Adv. Mater.*, 1998, **10**, 1036.
- 15 E. Ruiz-Hitzky, S. Letaief and V. Prévot, *Adv. Mater.*, 2002, **14**, 439.
- 16 Y. Fujimoto, A. Shimojima and K. Kuroda, *J. Mater. Chem.*, 2006, **16**, 986.

- 17 M. Choi, H. S. Cho, R. Sricastava, C. Venkatesan, D. H. Choi and R. Ryoo, *Nat. Mater.*, 2006, **5**, 718.
- 18 B. Ahlström, R. A. Thompson and L. Edebo, *APMIS*, 1999, **107**, 318.
- 19 Q. Huo, D. I. Margolese and G. D. Stucky, *Chem. Mater.*, 1996, **8**, 1147.
- 20 H. Yoshitake, *New J. Chem.*, 2005, **29**, 1107.
- 21 S. K. Medda, D. Kundu and G. De, *J. Non-Cryst. Solids*, 2003, **318**, 149.
- 22 S. Köytepe, T. Seçkin, N. Kıvrılcım and H. I. Adıgüzel, *J. Inorg. Organomet. Polym.*, 2008, **18**, 222.
- 23 C. Bonhomme, C. Coelho, N. Baccile, C. Gervais, T. Azaïs and F. Babonneau, *Acc. Chem. Res.*, 2007, **40**, 738.
- 24 K. H. Wu, T. C. Chang, C. C. Yang and G. P. Wang, *Thin Solid Films*, 2006, **513**, 84.
- 25 Q. Deng, B. Moore and K. A. Mauritz, *Chem. Mater.*, 1995, **7**, 2259.
- 26 A. Shimojima and K. Kuroda, *Chem. Rec.*, 2006, **6**, 53.
- 27 A. Shimojima, Y. Sugahara and K. Kuroda, *Bull. Chem. Soc. Jpn.*, 1997, **70**, 2847.
- 28 A. Shimojima and K. Kuroda, *Langmuir*, 2002, **18**, 1144.
- 29 W. C. Oliver and G. M. Pharr, *J. Mater. Res.*, 1992, **7**, 1564.
- 30 S.-q. Gong, L.-n. Niu, L. K. Kemp, C. K. Y. Yiu, H. Ryou, Y.-p. Qi, J. D. Blizzard, S. Nikonov, M. G. Brakkett, R. L. W. Messer, C. D. Wu, J. Mao, L. B. Brister, F. A. Rueggeberg, D. D. Arola, D. H. Pashley and F. R. Tay, *Acta Biomater.*, 2012, **8**, 3270.
- 31 (a) S. Q. Gong, J. Epasinghe, F. A. Rueggeberg, L. N. Niu, D. Mettenberg, C. K. Y. Yiu, J. D. Blizzard, C. D. Wu, J. Mao, C. L. Drisko, D. H. Pashley and F. R. Tay, *PLoS One*, 2012, **7**, e42355; (b) S. Q. Gong, D. J. Epasinghe, B. Zhou, L. N. Niu, K. A. Kimmerling, F. A. Rueggeberg, C. K. Y. Yiu, J. Mao, D. H. Pashley and F. R. Tay, *Acta Biomater.*, 2013, **9**, 6964.
- 32 A. M. Chen, M. Zhang, D. Wei, D. Stueber, O. Taratula, T. Minko and H. He, *Small*, 2009, **5**, 2673.